Magnetic Resonance of a Dextran-Coated Magnetic Fluid Intravenously Administered in Mice

L. M. Lacava,* Z. G. M. Lacava,* M. F. Da Silva,† O. Silva,‡ S. B. Chaves,* R. B. Azevedo,* F. Pelegrini,‡ C. Gansau,§ N. Buske,§ D. Sabolovic,¶ and P. C. Morais†

*Instituto de Biologia, Universidade de Brasília, 70910-900 Brasília (DF), Brazil; †Instituto de Física, Núcleo de Física Aplicada, Universidade de Brasília, 70919-970 Brasília (DF), Brazil; ‡Instituto de Física, Universidade Federal de Goiás, 74001-970 Goiânia (GO), Brazil; §Mediport Kardiotechnik GmbH, Wiesenweg 10, D-12247 Berlin, Germany; and ¶INSERM Unité 511, Faculté de Médicine Pitié-Salpêtrière, Paris Cedex 13-75643, France

ABSTRACT Magnetic resonance was used to investigate the kinetic disposition of magnetite nanoparticles (9.4 nm core diameter) from the blood circulation after intravenous injection of magnetite-based dextran-coated magnetic fluid in female Swiss mice. In the first 60 min the time-decay of the nanoparticle concentration in the blood circulation follows the one-exponential (one-compartment) model with a half-life of (6.9 $\pm$ 0.7) min. The X-band spectra show a broad single line at $g \approx 2$, typical of nanomagnetic particles suspended in a nonmagnetic matrix. The resonance field shifts toward higher values as the particle concentration reduces, following two distinct regimes. At the higher concentration regime (above 10^{14} cm^{-3}) the particle-particle interaction responds for the nonlinear behavior, while at the lower concentration regime (below 10^{14} cm^{-3}) the particle-particle interaction is ruled out and the system recovers the linearity due to the demagnetizing field effect alone.

INTRODUCTION

Magnetic resonance has been widely used in the investigation of nanomagnetic particles immersed in nonmagnetic matrices (Dormann et al., 1977; Komatsu et al., 1979; Morais et al., 1987). In recent years, the technique has been successfully used in the study of ionic (Tronconi et al., 1993) and surfacted (Sastry et al., 1995) magnetic fluids (MFs). Effects of particle concentration (Tronconi et al., 1993), ionic strength (Morais et al., 1995), and temperature (Morais et al., 1996) have been investigated using the nanomagnet as the resonant probe. Important information concerning the surface charge-discharge process (Morais et al., 1995), particle-particle interaction (Bakuzis et al., 1996), magnetic anisotropy (Saenger et al., 1998), and Brownian relaxation (Morais et al., 1997) in ionic MFs has been obtained through magnetic resonance investigations. In particular, magnetic resonance has been proved to be an excellent technique to investigate the relative contribution of both the anisotropy field and the exchange field of field-oriented nanomagnetic particles suspended in frozen nonmagnetic matrices (Bakuzis et al., 1999).

Despite the complexity of living beings, magnetic resonance has been recently used to investigate biomineralized nanomagnetite particles in the migratory ant *Pachycondyla marginata* abdomens (Wajnberg et al., 2000). The capability of the technique to sense as few as 100 pmol of nanomagnetic materials and to probe the size and the shape of nanomagnetic-based structures makes magnetic resonance a powerful tool in the investigation of nanomagnets introduced in living beings (Da Silva et al., 1997). In the present study a biocompatible MF sample based on dextran-coated nanomagnetite is given as an intravenous bolus dose to mice, while magnetic resonance is used to investigate the disposition of the nanomagnetic-based material out of blood circulation. The methodology for the kinetic data analysis, based on the magnetic resonance signal, is proposed in this study as well. Finally, it is shown that the time evolution (nanoparticle concentration decay) of the magnetic resonance field is in very good agreement with the kinetic analysis.

MATERIALS AND METHODS

The dextran-coated magnetic fluid (DC-MF) sample used to carry out the experiments was obtained by chemical co-precipitation of Fe(II) and Fe(III) ions in alkaline medium to produce 9.4 nm average-diameter magnetite particles, following surface coating with a single layer of dextran. After surface coating the nanomagnetite particles with dextran, the DC-MF sample was diluted in water and stabilized at neutral pH, in a concentration of $\sim 4.9 \times 10^{16}$ particle/cm^3. The interest in this sample is mainly due to the extremely reduced toxicity it presents when in vivo tests are performed (Lacava et al., 1999). In order to carry out the resonance experiments 100 μl of the DC-MF sample was given as an intravenous bolus dose to female Swiss mice (average of 30 g in weight). The DC-MF sample was administered to 36 animals and $\sim$10 μl of blood was collected from a set of three animals every 5 min after administration of the DC-MF sample, up to 60 min. The resonance data (area under the absorption curve and resonance field) were averaged out at each time point using three animals. Three extra animals were not treated with the DC-MF sample and were used as control; 10-μl blood samples from the control were used in the experiment, before (pure) and after mixing with the DC-MF sample. The DC-MF samples were administered through the animal's tail vein. Likewise, all the blood samples (total blood) were collected by tail-bleeding the animals. The blood samples collected from the animals were transferred to heparinized sample holders. Different amounts of the

Received for publication 16 October 2000 and in final form 24 January 2001.

Address reprint requests to Dr. P. C. Morais, Instituto de Física, Núcleo de Física Aplicada, Universidade de Brasília, 70919-970 Brasília (DF), Brazil. Tel.: 55-61-273-6655; Fax: 55-61-272-3152; E-mail: pcmor@fis.unb.br.

0006-3495/01/05/2483/04 $2.00

DC-MF sample were mixed with the blood samples in order to obtain the calibration curve, i.e., the area under the resonance absorption curve versus the nanoparticle concentration, in the range of 5×10^{12} to 5×10^{15} particle/cm^3. Room-temperature magnetic resonance spectra were obtained from the blood samples using Bruker ESP-300 equipment tuned to ~9.4105 GHz. Indeed, three different samples were investigated in this study: the blood samples collected from the animals (MFB) some time after (5–60 min) intravenous administration of the magnetite-based DC-MF sample, the DC-MF samples mixed with blood from the control (MFM), and the pure blood samples collected from the control (PBC).

RESULTS AND DISCUSSION

Fig. 1 shows typical room-temperature resonance spectra (first derivative of the absorption curves) of the MFB samples as a function of time (5, 30, and 60 min). The MFM samples presented similar magnetic resonance spectra (not shown). The PBC samples showed no typical resonance signal, even when the equipment sensitivity was set two orders of magnitude higher than the highest sensitivity (60 min spectrum) used to obtain the spectra shown in Fig. 1. Note in Fig. 1 that the signal-to-noise ratio decreases as the resonance field shifts to higher values (see vertical bars), i.e., as the blood collecting time increases from 5 to 60 min. After 60 min the concentration of the nanomagnetite particles in the blood circulation has been reduced by about three orders of magnitude.

Open circles in Fig. 2 represent the time-decay (disposition) of the nanomagnetite particle concentration in the MFB samples. Determination of the nanoparticle concentration in the MFB samples is obtained from the area under the magnetic resonance absorption curve. Calibration involving the area under the magnetic resonance absorption curve versus nanomagnetite concentration was previously performed using the MFM samples, as shown in the inset of Fig. 2. Dilution of the original DC-MF sample (4.9×10^{16} particle/cm^3) in water was also realized (resonance data not shown) in order to obtain DC-MF samples in the same particle concentration range as the calibration curve (Fig. 2, *inset*). When compared to the MFM samples the resonance linewidth of the water-diluted samples present deviation of $<1\%$, indicating similar chemical stability of the dextran-coated nanomagnetite particles after dilution in both media (blood and water). The experimental data (*filled circles*) in the calibration curve (Fig. 2, *inset*) were fitted by the solid straight line with a slope of $(2.4 \pm 0.1) \times 10^{15}$ particle/cm^3. In the calibration data (Fig. 2, *filled circles*) the vertical error bar matches the symbol size while the horizontal error bar is ~60% of the symbol size. It is clear from the semi-log plot (Fig. 2) that the kinetic of the nanomagnetite disposition is first-order and well-described by the one-compartment model (Nony et al., 1998). Then, the nanomagnetite

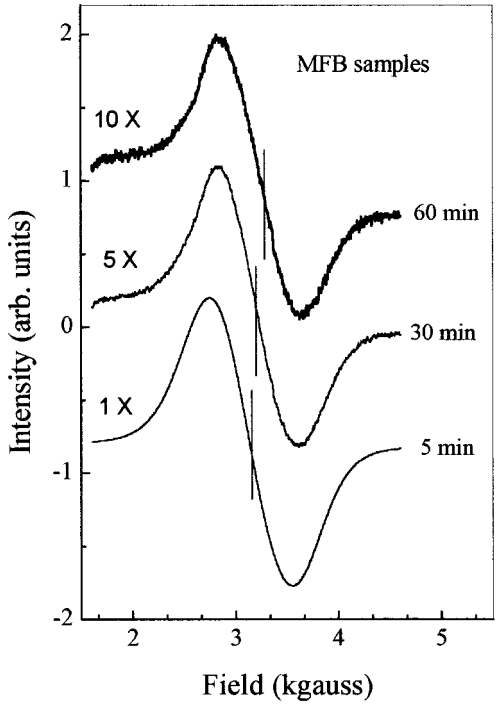

FIGURE 1 Typical magnetic resonance spectra taken from the blood samples collected from the animals after injection of the magnetic fluid bolus dose (MFB samples). The curves represent the first derivative of the X-band absorption spectra. The vertical bar represents the resonance field position associated to the spectrum.

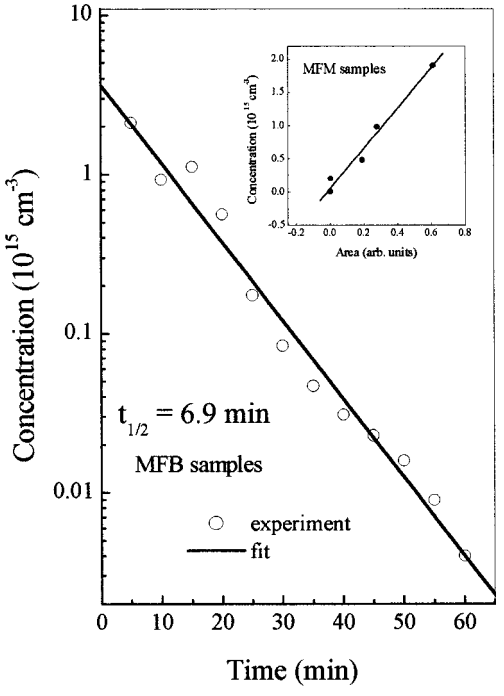

FIGURE 2 Nanomagnetite concentration-time curve following intravenous administration of the magnetic fluid bolus dose. The solid line represents a one-exponential (one-compartment) model to data. The inset shows the calibration curve obtained from the area under the magnetic resonance absorption spectra.

particle concentration, $C(t)$, in blood at time t, is written as:

$$C(t) = C_0 \exp(-kt) \quad (1)$$

where C_0 and k are the nanomagnetite concentration at $t = 0$ and the constant of transfer of nanomagnetite out from the blood circulation, respectively. The solid line in Fig. 2 is the best fit of the data (*open circles*) using Eq. 1, with $C_0 = (3.5 \pm 0.4) \times 10^{15}$ particle/cm^3 and $k = (0.10 \pm 0.01)$ min^{-1}. Note that $k = (0.10 \pm 0.01)$ min^{-1} defines the slope of the straight line in the semi-log plot of Fig. 2. The vertical error bar associated with the lowest concentration time point matches the symbol size (*open circles* in Fig. 2), while the vertical error bar associated with the highest concentration time point is ~20% of the symbol size. The horizontal error bar in Fig. 2 (*open circles*) is about half the symbol size. The half-life associated to the nanomagnetite disposition is given by $t_{1/2} = 0.693/k = (6.9 \pm 0.7)$ min. Furthermore, the $C_0 = (3.5 \pm 0.4) \times 10^{15}$ particle/cm^3 value obtained from the fitting (see Fig. 2) is in very good agreement with the expected value of 3.1×10^{15} particle/cm^3, calculated from the dilution of the bolus dose (100 μl at 4.9×10^{16} particle/cm^3) in the mouse average blood volume (1.5 ml).

Open circles in Fig. 3 represent the resonance field (H_R) versus the inverse of the nanoparticle concentration ($1/C$). The vertical error bar matches the symbol size (*open circles*), while the horizontal error bar is only ~5% of the symbol size. The description of the resonance field dependence upon the nanomagnetic particle concentration, C, starts with the basic resonance equation, i.e., $H_{EFF} = \omega_R/\gamma$, where H_{EFF} is the effective field at the resonance center, ω_R is the microwave frequency, and γ is the gyromagnetic ratio. At low particle concentration the effective field is mainly a combination of the external field (H_E), the exchange field (H_X), the anisotropy field (H_K), and the demagnetizing field (H_D), i.e., $H_{EFF} = H_E + H_X + H_K + H_D$ (Bakuzis et al., 1999). Only the demagnetizing field depends upon the nanoparticle concentration. At the resonance condition, the external field matches the resonance field ($H_E = H_R$) and the basic resonance equation is rewritten as $H_R = H_0 - H_D$, with $H_0 = \omega_R/\gamma - H_X - H_K$. The demagnetizing field of an assembly of isolated spherical nanoparticles in a magnetically inert matrix, however, is given by $H_D = (4\pi/3)[(1/p) - 1]M$, where M is the magnetization associated to the nanomagnetic particle and p is the volumetric packing fraction of the nanomagnetic material in the matrix (Kneller, 1969). The relationship between p and C is $p = \pi D^3 C/6$, where D is the nanoparticle diameter. Therefore, at the low-concentration end the relationship between the resonance field (H_R) and the nanoparticle concentration (C) would be written as $H_R = h_0 + k_1/C$, where h_0 and k_1 are fitting parameters. The data in Fig. 3 (*open circles*), however, show a linear relationship between H_R and $1/C$ only at nanoparticle concentration below ~10^{14} cm^{-3}. Above 10^{14} cm^{-3} particle-particle (dipole) interaction plays a key role in the H_R versus $1/C$ curve, and thus needs to be taken into account.

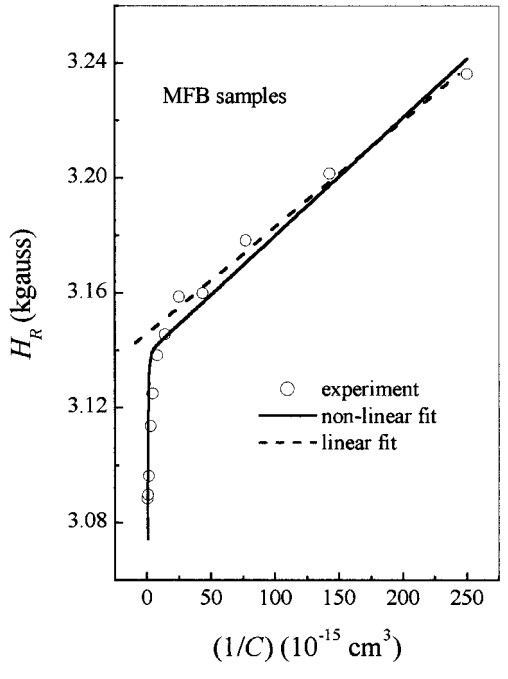

FIGURE 3 Resonance field as a function of the inverse of particle concentration. Open circles are the experimental data. The solid line represents the best fit using the nonlinear model (Eq. 2), while the dashed line represents the fitting above 10^{-14} cm^3, using the linear model.

Inclusion of the particle-particle interaction in the description of the H_R versus $1/C$ curve assumes the following relationship between the resonance field shift (δH_R) and the resonance linewidth (ΔH_R): $\delta H_R \approx \Delta H_R{}^2$ (Nagata and Ishihara, 1992). Description of the resonance linewidth as a function of the nanoparticle concentration has been successfully achieved by $\Delta H_R \approx C \tanh(KC^2)$, where K depends upon both the temperature and the magnetic moment of the particle (Morais et al., 1996). Therefore, the description of the H_R versus $1/C$ data, including both the demagnetizing field and the particle-particle interaction, reads:

$$H_R = H_0 + K_1/C - K_2 C^2 \tanh^2(K_3 C^2) \quad (2)$$

where H_0 and K_j ($j = 1, 2, 3$) are fitting parameters. The solid line in Fig. 3 represents the best fit of the data according to Eq. 2. The dashed line in Fig. 3 represents the best fit of the experimental data, for nanoparticle concentration below 10^{14} cm^{-3}, using only the two first terms on the right-hand side of Eq. 2. Though particle-particle interaction is extremely important in determining the particle concentration dependence of the resonance field, it does not have any influence upon the concentration dependence of the area under the resonance absorption curve. This is a very important point, as far as the use of the magnetic resonance to monitor the nanoparticle concentration in biological systems is concerned.

CONCLUSIONS

In summary, magnetic resonance has been proposed as a spectroscopic technique in the study of the kinetic disposition of nanomagnetite-based dextran-coated magnetic fluid intravenously administered in mice. The resonance data show a nanoparticle concentration decay of about three orders of magnitude one hour after intravenous injection of a bolus dose. The data show a first-order kinetic well-described by the one-compartment model, with a half-life of (6.9 ± 0.7) min. The resonance field dependence of the nanoparticle concentration shows a strong nonlinear behavior as the particle concentration goes above 10^{14} cm^{-3}. Such nonlinear behavior was explained in terms of the dipolar interaction between nanomagnetite particles. Despite the complexity of the particle-particle interaction and in contrast to its influence upon the magnetic resonance field, the intensity of the resonance signal (area under the absorption curve) was successfully used to probe the time-decay of the nanoparticle concentration in blood circulation, in a wide range of particle concentration.

This work was partially supported by the Brazilian agencies FAP-DF and FINATEC, and by the International Brazilian/French (CNPq/INSERM) cooperation agreement.

REFERENCES

Bakuzis, A. F., P. C. Morais, and F. Pelegrini. 1999. Surface and exchange anisotropy fields in $MnFe_2O_4$ nanoparticles: size and temperature effects. *J. Appl. Phys.* 85:7480–7482.

Bakuzis, A. F., P. C. Morais, and F. A. Tourinho. 1996. Investigation of the magnetic anisotropy in manganese ferrite nanoparticles using magnetic resonance. *J. Magn. Reson. A.* 122:100–103.

Da Silva, M. F., F. Gendron, J. C. Bacri, J. Roger, J. N. Pons, M. Rabineau, D. Sabolovic, and A. Halbretch. 1997. Quantification of maghemite nanoparticles in biological media by ferromagnetic resonance and its alteration by conjugation with biological substances. *In* Scientific and Clinical Applications of Magnetic Carriers. U. Hafeli, W. Schutt, J. Teller, and M. Zborowski, editors. Plenum Press, New York 171–176.

Dormann, J. L., P. Gibart, G. Suran, and C. Sella. 1977. Magnetic properties of granular Fe-SiO_2. *Physica B & C.* 86:1431–1433.

Kneller, E. 1969. Fine particle theory. *In* Magnetism and Metallurgy, Vol. 1. A. E. Berkowitz and E. Kneller, editors. Academic Press, New York. 365–471.

Komatsu, T., N. Soga, and M. Kunugi. 1979. ESR study of $NiFe_2O_4$ precipitation process from silicate-glasses. *J. Appl. Phys.* 50: 6469–6474.

Lacava, L. M., L. P. Silva, S. B. Chaves, G. S. Correia, Z. G. M. Lacava, and R. B. Azevedo. 1999. Morphological effects of a dextran-magnetic-fluid in the liver. *Acta Microscopica Suppl. C.* 8:745–746.

Morais, P. C., M. C. F. L. Lara, and K. Skeff Neto. 1987. Electron spin resonance in superparamagnetic particles dispersed in a non-magnetic matrix. *Phil. Mag. Lett.* 55:181–183.

Morais, P. C., M. C. F. L. Lara, A. L. Tronconi, F. A. Tourinho, A. R. Pereira, and F. Pelegrini. 1996. Magnetic particle-particle interaction in frozen magnetic fluids. *J. Appl. Phys.* 79:7931–7935.

Morais, P. C., F. A. Tourinho, G. R. R. Gonçalves, and A. L. Tronconi. 1995. Ionic strength effect on magnetic fluids: a resonance study. *J. Magn. Magn. Mater.* 149:19–21.

Morais, P. C., A. L. Tronconi, F. A. Tourinho, and F. Pelegrini. 1997. Investigation of the Brownian relaxation and hydrodynamic radius in magnetic nanoparticles. *Solid State Commun.* 101:693–697.

Nagata, K., and A. Ishihara. 1992. ESR of ultrafine magnetic particles. *J. Magn. Magn. Mater.* 104:1571–1573.

Nony, P., M. Cucherat, and J.-P. Boissel. 1998. Revisiting the effect compartment through timing errors in drug administration. *Trends Pharmacol. Sci.* 19:49–54.

Saenger, J. F., K. Skeff Neto, P. C. Morais, M. H. Sousa, and F. A. Tourinho. 1998. Investigation of the anisotropy in frozen nickel ferrite ionic magnetic fluid using magnetic resonance. *J. Magn. Reson.* 134: 180–183.

Sastry, M. D., Y. Babu, P. S. Goyal, R. V. Mehta, R. V. Upadhyay, and D. Srinivas. 1995. Electron magnetic resonance of ferrofluids: evidence for anisotropic resonance at 77 K in samples cooled in a magnetic field. *J. Magn. Magn. Mater.* 149:64–66.

Tronconi, A. L., P. C. Morais, F. Pelegrini, and F. A. Tourinho. 1993. Electron paramagnetic resonance study of ionic water-based manganese ferrite ferrofluids. *J. Magn. Magn. Mater.* 122:90–92.

Wajnberg, E., D. Acosta-Avalos, L. J. El-Jaick, L. Abraçado, J. L. A. Coelho, A. F. Bakuzis, P. C. Morais, and D. M. S. Esquivel. 2000. Electron paramagnetic resonance study of the migratory ant *Pachycondyla marginata* abdomens. *Biophys. J.* 78:1018–1023.